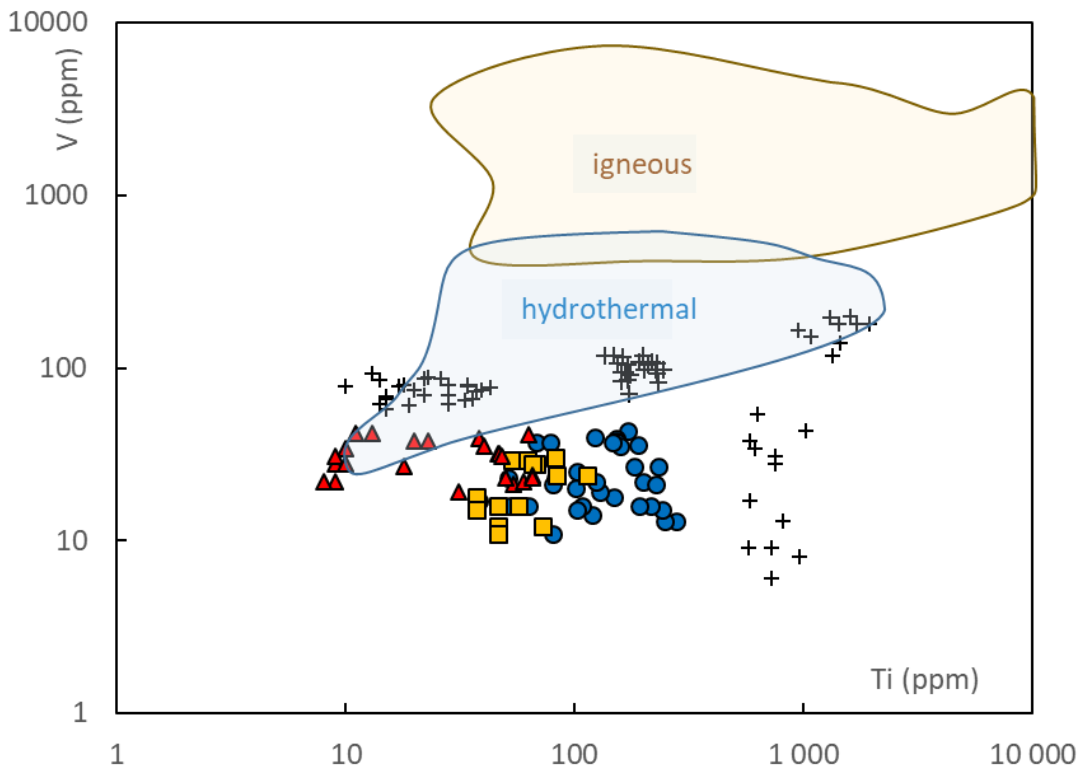
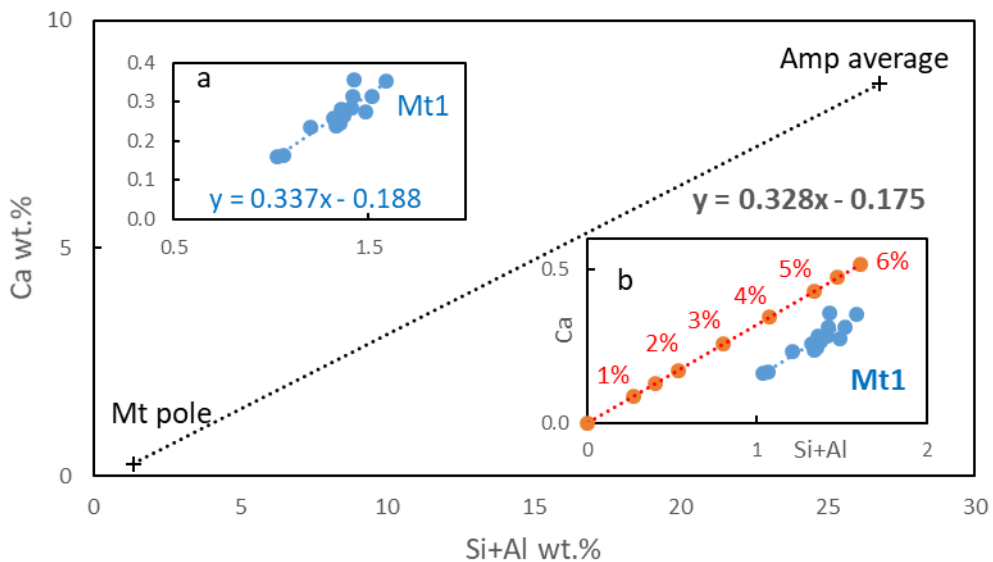


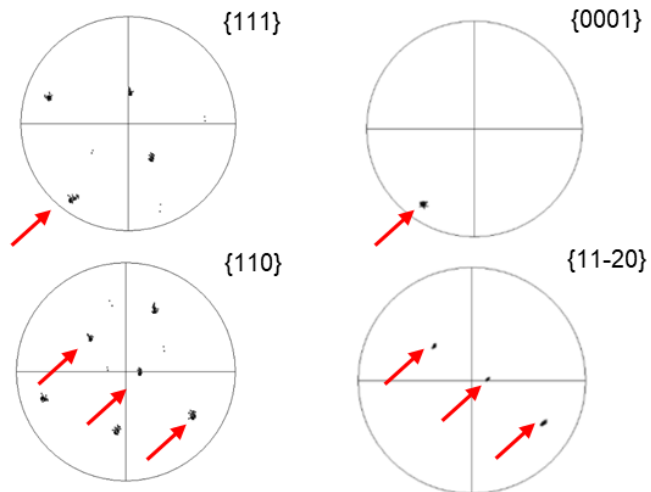
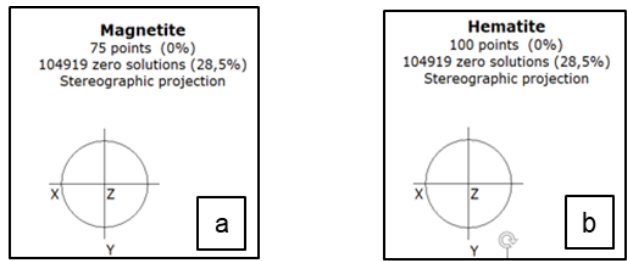
Supplementary Figure S1. (a-e) WDS X-Ray maps of selected elements in a magnetite grain from sample TAK-Z3. As observed in magnetite from sample TAK-Z1 (Figure 7), magnetite Mt1 contains higher Si, Al and Ca than magnetite Mt2. Mt3 bands have the highest Fe and the lowest Si, Al and Ca contents. The difference in Mg composition is not visible on the Mg X-Ray map although clearly distinct in EMPA data (Table 2).



Supplementary Figure S2. Discrimination diagram of V vs Ti. Most of the Takab massive magnetite Mt1 (blue circles), Mt2 (yellow squares) and Mt3 (red triangles) plot outside the hydrothermal field due to a very low V content. Therefore, this discriminating diagram does not give any reliable information. Crosses refer to banded, nodular and disseminated Takab magnetite from [8, 28]. Most of these magnetite data plot in the hydrothermal field. Hydrothermal and magmatic domains after [34].



Supplementary Figure S3. Binary plot of magnetite Mt1 and co-existing amphibole from sample TAK-Z1. To examine the possible presence of amphibole inclusions in magnetite, we have checked whether the amphibole will be on the continuation trend of the magnetite compositions. The slopes of the compositions of magnetite ($y = 0.337x - 0.188$, insert a) and the line connecting pure magnetite and amphibole average composition ($y=0.328x-0.175$) are similar in terms of Ca/(Si+Al). This allowed to approximate up to 6% the amphibole component in the magnetite compositions (insert b). However, this admixture overestimates the observed Ca content of magnetite for a given (Si + Al) content.



Supplementary Figure S4. Pole figures of selected area of magnetite Mt3 (a) close to relict hematite (b) in sample TAK-Z1 showing coincidence of orientation between the planes $\{0001\}_{\text{Hem}}/\{111\}_{\text{Mt}}$ and $\{11-20\}_{\text{Hem}}/\{110\}_{\text{Mt}}$, which results from constraints imposed by the similarity between the crystal structures of magnetite and hematite.

Table S1. Composition (in wt. %) of feldspar from Takab host amphibolite and iron ore.

	host		iron ore	
	Albite		Albite	
SiO ₂	66.77	66.73	66.24	67.17
TiO ₂	0.00	0.01	0.00	0.03
Al ₂ O ₃	21.45	20.93	21.07	20.56
FeO	0.35	0.42	0.37	0.25
MnO	0.00	0.00	0.06	0.02
MgO	0.00	0.00	0.00	0.04
CaO	1.54	1.48	1.63	1.34
Na ₂ O	10.41	10.95	10.88	11.05
K ₂ O	0.19	0.26	0.26	0.19
Total	100.72	100.77	100.52	100.65
% Ab	91.4	91.7	92.7	92.7
% An	7.5	6.9	6.2	6.2
% Or	1.1	1.4	1.1	1.1

Table S2. Fe, O (wt. %) and trace element (ppm) composition of magnetite from the Takab iron ore samples.

Sample	Mt type	Fe	O	Si	Ti	Al	Mn	Mg	Ca	V
TAK-Z1	Mt1	68.33	29.33	12779	276	3103	288	1306	3529	13
		68.92	29.26	11320	119	2056	274	807	2383	14
		69.48	29.32	8899	82	1428	289	1003	1606	23
		68.48	29.48	11102	170	2497	242	1265	2810	43
		68.83	29.46	9834	122	2218	198	833	2348	40
		69.16	29.44	9021	80	1653	242	1258	1653	21
		67.76	29.74	11758	181	2532	250	1543	3578	27
		67.26	29.15	11101	149	2650	281	1882	2661	18
		67.53	28.99	11738	51	2380	277	1401	2850	23
		67.38	29.54	10600	102	2644	273	1471	2597	25
		66.74	29.23	10903	129	2635	246	1074	2443	19
		67.87	29.61	11546	101	2633	273	952	3134	20
	Mt2	70.44	28.27	4395	83	1060	305	560	1349	24
		69.97	28.81	4840	37	995	220	414	1127	18
		69.52	28.73	4264	72	947	220	433	1358	12
		69.26	28.70	3846	114	1120	161	234	1322	24
	Mt3	71.30	28.59	107	9	312	318	40	296	22
		71.20	29.07	120	46	434	222	-	228	32
		70.72	28.47	426	63	339	287	51	305	41
		71.10	28.01	62	11	203	405	-	346	42
		70.78	28.76	200	-	463	245	43	426	27
		71.16	28.53	299	9	233	190	-	379	28
		71.05	27.98	545	38	260	238	43	484	39
		71.29	28.60	549	40	256	519	26	409	35
		69.89	28.55	10	10	188	181	-	194	34
		70.18	28.38	22	-	226	173	55	225	29
		70.57	28.53	119	9	193	192	65	245	31
		70.48	28.55	103	23	187	166	71	220	38
TAK-Z3	Mt1	67.70	29.29	12740	124	3231	254	1738	3426	22
		68.24	29.31	11739	80	2945	194	1038	2809	11
		68.41	29.46	11369	63	2597	197	799	2422	16
		67.79	29.87	13503	68	3224	250	1500	3575	37
		69.14	29.61	10879	38	1978	219	1143	1978	17
		68.46	29.52	12707	52	2795	216	1399	3273	16
		69.18	29.17	9769	78	1745	215	614	1966	37
		67.70	29.55	13115	153	3480	246	1653	3531	39
		67.26	29.34	13732	246	3437	217	1169	3356	13
		68.74	29.19	9893	153	2227	181	677	2200	38
		67.87	29.52	12009	189	2935	205	1410	3277	36
		68.65	29.20	10227	155	2239	205	1214	2764	37
		67.66	28.87	12475	240	3074	213	1228	3276	15
		67.50	29.60	13780	214	3643	258	1610	3540	16
		69.12	29.38	11335	199	2511	229	936	2520	22
		68.17	29.60	12938	227	3377	220	1663	2973	21
		68.57	29.19	10261	158	2248	212	1302	2045	35
		67.92	29.55	11133	191	2796	224	1235	2582	16
		67.96	29.58	12279	147	2824	222	1425	3004	37
		67.62	29.56	11868	232	2911	262	1509	3290	27
		68.05	29.70	10956	108	2557	249	1410	2762	16

	68.97	29.41	10411	102	2380	237	1456	2449	15	
Mt2	69.68	29.00	5314	53	1313	222	597	1636	29	
	69.63	28.85	5888	37	1334	230	724	1810	15	
	69.76	28.83	5481	62	759	221	825	1418	29	
	69.26	29.16	7170	46	1621	238	1004	2226	12	
	69.50	29.08	5055	82	1213	196	877	1322	30	
	69.81	29.22	6384	68	1272	243	1064	1940	28	
	70.21	29.05	3949	57	886	276	342	1150	16	
	70.08	28.56	4372	46	1122	309	575	1302	16	
	69.48	29.08	5701	46	1360	242	927	2002	11	
	69.92	29.22	4988	65	1017	225	810	1808	28	
porous	Mt3	71.24	28.63	33	8	200	174	70	640	nd
		70.73	29.66	1070	11	372	292	46	702	nd
		70.39	28.43	12	-	201	207	24	824	nd
		71.05	28.64	795	-	279	180	-	316	nd
		71.06	28.27	625	17	246	182	54	313	nd
		71.54	28.50	969	10	468	228	-	320	nd
		71.35	28.64	195	8	211	169	61	316	nd
		70.95	28.75	998	13	247	148	58	350	nd
TAK-Z4	Mt3	71.19	28.62	141	8	175	223	20	249	22
		70.42	28.69	452	10	519	176	47	435	28
		71.14	28.68	620	13	296	204	89	359	42
		71.44	28.59	55	20	105	133	87	244	38
		70.95	28.48	774	54	254	238	34	574	21
		70.90	28.43	159	31	189	194	100	335	19
		71.00	28.56	369	60	229	208	54	341	22
		71.26	28.90	884	47	315	203	18	403	32
		70.28	29.45	879	65	205	101	59	494	24
		71.34	28.83	374	48	222	137	77	390	31
		71.79	30.29	408	50	223	192	87	797	23
		71.41	28.71	409	65	219	143	67	718	23
		71.46	28.54	52	18	173	261	36	228	27
	Mt1	67.89	29.31	11122	211	2304	198	1006	1871	nd
		67.19	29.18	9630	156	2624	286	1794	2501	nd
		67.34	29.57	11941	427	2619	271	1155	3821	nd
		67.49	29.02	8274	321	2143	233	976	2980	nd
		68.72	27.98	9300	149	1617	331	1710	1760	nd
		67.78	28.69	8546	267	2195	289	825	2867	nd
		67.64	29.27	9015	335	2294	368	881	3190	nd
		66.87	29.50	11705	474	2773	254	1449	3405	nd
	Mt2	69.49	28.80	3028	73	963	216	440	1044	nd
		69.89	29.11	3873	121	1015	193	266	1155	nd
		69.43	27.67	3149	106	1301	273	205	1018	nd
		70.05	28.86	4045	122	973	217	469	1785	nd
		69.02	28.69	3584	95	818	222	553	1062	nd
		69.92	28.74	3623	104	842	214	361	1087	nd

(-) = below detection limit. V not determined in magnetite Mt3porous from TAK-Z1 and in magnetite from TAK-Z4.

Calculation of magnetite formulas and Fe²⁺/Fe³⁺ partitioning

As there is no direct measurement of the oxidation of Fe with the electron microprobe, all Fe is considered as Fe²⁺.

The amount of Fe³⁺ is calculated assuming a perfect stoichiometric formula with three cations and four oxygens.

The analysis is first normalized to 3 cations, then the oxygen is assigned to each cations according to valence and the oxygen is summed.

If the oxygen sum is < 4, then an appropriate amount of oxygen is added to bring the sum at 4.

For each amount added, twice that amount of Fe is converted from Fe²⁺ to Fe³⁺.

(Being aware that this method is sensitive to error's in the analyses of the major elements).

Table S3. Average formation temperature for the Takab magnetite.

Sample	Mt type	T°C	range	n analyses
TAK-Z1	Mt1	595	560-620	14
TAK-Z1	Mt2	503	468-529	5
TAK-Z1	Mt3	440	420-475	12
TAK-Z3	Mt1	598	537-625	23
TAK-Z3	Mt2	553	493-549	10
TAK-Z3	Mt3 porous	321	265-346	8
TAK-Z3	Mt3	380	329-415	13
TAK-Z4	Mt1	456	436-475	8
TAK-Z4	Mt2	439	431-452	6

Temperatures calculated using the $T_{\text{Mg-mag}}$ thermometer from [40].